Spin transition with a large thermal hysteresis near room temperature in a water solvate of an iron(III) thiosemicarbazone complex†

Sébastien Floquet,[a] Marie-Laure Boillot,*[a] Eric Rivière,[a] François Varret,[b] Kamel Boukheddaden,[b] Denis Morineau[c] and Philippe Négrier[d]

[a] *Laboratoire de Chimie Inorganique (CNRS UMR 8613), Université Paris-Sud, 91405, Orsay, France. E-mail: mboillot@icmo.u-psud.fr*
[b] *Laboratoire de Magnétisme et d'Optique (CNRS UMR 8634), Université de Versailles Saint-Quentin, 78035, Versailles, France*
[c] *Laboratoire de Chimie-Physique (CNRS UMR 8611), Université Paris-Sud, 91405, Orsay, France*
[d] *Laboratoire C.P.M.O.H., Université de Bordeaux I, 33350, Talence, France*

Received (in Montpellier, France) 31st July 2002, Accepted 2nd October 2002
First published as an Advance Article on the web 6th January 2003

The magnetic properties of the monohydrated ferric complex Li[Fe(5Brthsa)$_2$]·H$_2$O (H$_2$-5Brthsa = 5-bromosalicylaldehyde thiosemicarbazone) have been investigated by SQUID and Mössbauer measurements. The $S = 1/2 \leftrightarrow S = 5/2$ spin transition of the ferric ion is accompanied by a quite broad hysteresis ($\Delta T = 39$ K) centred around 313 K. The spin states involved are characterised by the quadrupole splittings $\Delta E_Q(^2T_2) = 2.584 \pm 0.002$ mm s^{-1} and $\Delta E_Q(^6A_1) = 0.338 \pm 0.006$ mm s^{-1} and the isomer shifts δ^{IS} ($^2T_2$) $= +0.262 \pm 0.001$ mm s^{-1} and δ^{IS} ($^6A_1$) $= +0.294 \pm 0.002$ mm s^{-1} at 77 and 360 K, respectively. A powder X-ray diffraction study at various temperatures demonstrates the occurrence of a crystallographic first-order phase transition of the lattice coupled to the spin conversion. The enthalpy and entropy variations associated with the transition have been estimated from DSC measurements at $\Delta H = 5.7 \pm 0.5$ kJ mol^{-1} and $\Delta S = 18 \pm 2$ J mol^{-1} K^{-1}. The existence of a crystallographic first-order phase transition associated to the spin crossover is consistent with the cooperative character of the process. This phase transformation might originate from the modification of the extended hydrogen-bond network.

Since the discovery of the spin-crossover phenomenon in tris(*N*,*N*-dialkyldithiocarbamato) iron(III) complexes[1] numerous investigations have been devoted to this field of molecular magnetism.[2,3] Discontinuous spin-crossover transformations can occur in the solid state when strong intermolecular interactions give rise to a cooperative mechanism. A number of discontinuous transitions with thermal hysteresis have been reported for iron(II) complexes (see for instance refs. 4 to 6). The observation of such transitions makes the materials potential candidates for information storage and display devices.[7]

Iron(III) complexes undergoing a thermal spin-crossover between the high-spin (HS, $S = 5/2$) and the low-spin (LS, $S = 1/2$) states are usually characterised by small changes in the molecular volume and continuous transformation over a wide range of temperature.[1,8,9] A unique class of iron(III) thiosemicarbazone complexes exhibits the full range of spin-crossover phenomenon in the solid state. Continuous, discontinuous and also two-step spin-crossover transformations have been described by Zelentsov *et al.*[10] To our knowledge, the only other examples of $S = 5/2 \leftrightarrow S = 1/2$ discontinuous transitions showing a thermal hysteresis are those reported in the case of the related ferric complexes [Fe(Hthpu)(thpu)] and [Fe(HL)$_2$]Cl (where H$_2$thpu and H$_2$L are the protonated forms of pyruvic acid thiosemicarbazone and pyridoxal thiosemicarbazone, respectively) or Schiff-base ferric complexes.[11,12]

In the course of the work already engaged with ferric complexes on the so-called ligand-driven light-induced spin change[13] effect, we have chosen to functionalise a thiosemicarbazone ligand by a photosensitive group. As the first step of this synthetic work, we have prepared a thiosemicarbazone ferric complex previously described in the literature in a non-solvated form, *viz.* Li[Fe(5Brthsa)$_2$] (R-thsa denotes a R-substituted salicylaldehyde thiosemicarbazone).[14,15] A monohydrated complex has been isolated in contrast to the published results. The investigation of the electronic properties of this solid compound has revealed a discontinuous spin transition with a thermal hysteresis centred around room temperature.

We report below a study of this discontinuous transition of Li[Fe(5Brthsa)$_2$]·H$_2$O based on SQUID, ^{57}Fe Mössbauer and differential scanning calorimetry measurements. The temperature dependence of the powder X-ray diffraction patterns has been examined in order to clarify the origin of a thermal hysteresis near room temperature.

Results and Discussion

Both a crystalline and a ^{57}Fe-enriched sample, denoted **1** and **2**, respectively, were examined.

Syntheses and characterisations

Despite our efforts, we have been unable to grow suitable single crystals for X-ray structure determination. Elemental

† Dedicated to the memory of Professor Olivier Kahn.

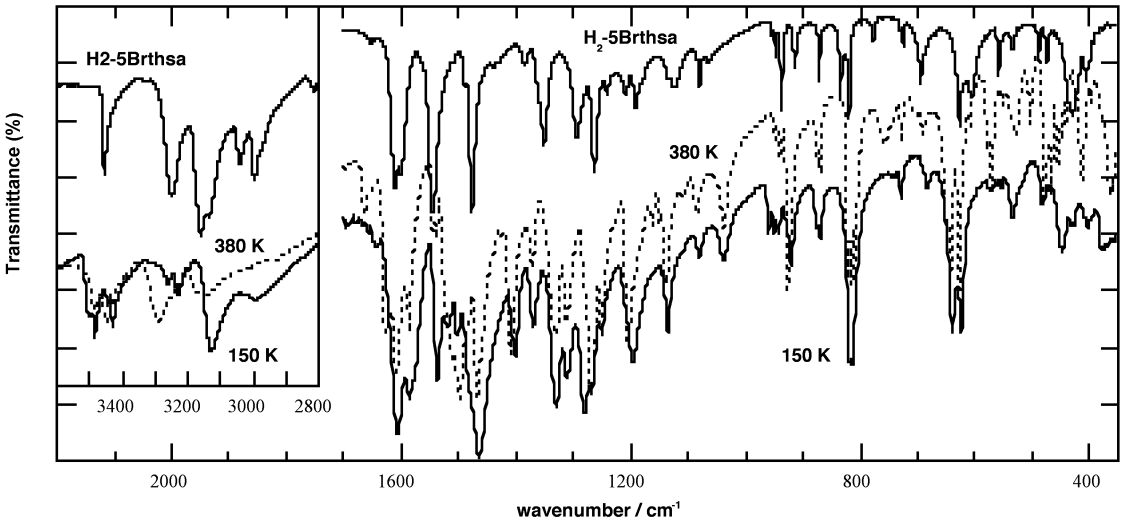

Fig. 1 FTIR spectra of H_2-5Brthsa and Li[Fe(5Brthsa)$_2$]·H_2O (**1**, T = 150 and 380 K) dispersed into a KBr pellet.

analysis and ES-MS spectrometry confirm that the complex salt studied here is Li[Fe(5Brthsa)$_2$]·H_2O. The formation of a water solvate, which is fully supported by FTIR measurements (*vide infra*), contrasts with the literature data.[14,16,17] The anhydrous form that has been previously described most likely results from slightly different experimental conditions.

Several details regarding the molecular structure can be drawn from the comparison of the temperature-variable FTIR data of **1** to those of the uncoordinated ligand.[18a,b] In Fig. 1 are displayed the IR spectra of Li[Fe(5Brthsa)$_2$]·H_2O (at 150 and 380 K) and H_2-5Brthsa. The complexation of the metal ion is accompanied by the loss of the NH proton of the –NH–(C=S)NH_2 group (disappearance of ν_{NH} and $\nu_{C=S}$ at 3161 and 1064 cm^{-1}, respectively) and the subsequent formation of a –N=C(–S–)NH_2 group (new N=C band in the spectral region of 1630–1595 cm^{-1}).[18b,d] As expected for chelating thiosemicarbazone,[18e,f] the frequencies corresponding to $\nu_{N=C}^{azomethyne}$, $\nu_{amide\ II}$, ν_{CO} and ν^{s}_{CS} of **1** appear to be negatively ($\nu_{N=C}^{azomethyne}$, $\nu_{amide\ II}$, ν^{s}_{CS}) or positively (ν_{CO}) shifted with regards to the free ligand, therefore indicating the coordination of the ferric ion to the O, N, and S atoms. This observation is also consistent with the marked changes observed in the spectrum (see, for example, the $CN_{azomethyne}$ and CO bands in Fig. 1) when the temperature varies between 150 and 380 K following the spin transformation of the metal ion (*vide infra*). It can be inferred from these observations that the ligand donor atoms [ONS] chelate the ferric ion in a tridentate manner as in a number of related anionic ferric complexes.[19] The pseudo-octahedral structure we propose for Fe(5Brthsa)$_2^-$, a very common stereochemistry,[20] is represented in Fig. 2.

As previously mentioned, the ferric salt was prepared with one water molecule of crystallization that is very likely held to the complex by strong hydrogen bonds. This assertion is supported by the appearance, in the spectral region of 3550–3400 cm^{-1} (inset in Fig. 1), of broad and rather intense absorption bands assigned to the ν_{OH} modes of water.[18b,c,g] The IR spectrum at 150 K shows a fine structure of these bands. In comparison to the free ligand data, the set of broad bands assigned to the ν_{NH2} modes of thiosemicarbazone is found to be shifted at high and low temperatures for complex **1** but spreads over the same spectral range (3400–3000 cm^{-1}). In the spectra of **1** recorded at decreasing temperatures down to 150 K, the frequencies of the more intense ν_{OH} and ν_{NH2} peaks are shifted toward higher (ν_{OH}) or lower (ν_{NH_2}) values. These changes might suggest that, at low temperature, hydrogen bonds involving OH groups are weakened whereas those arising from NH_2 groups are reinforced in the LS state. It follows

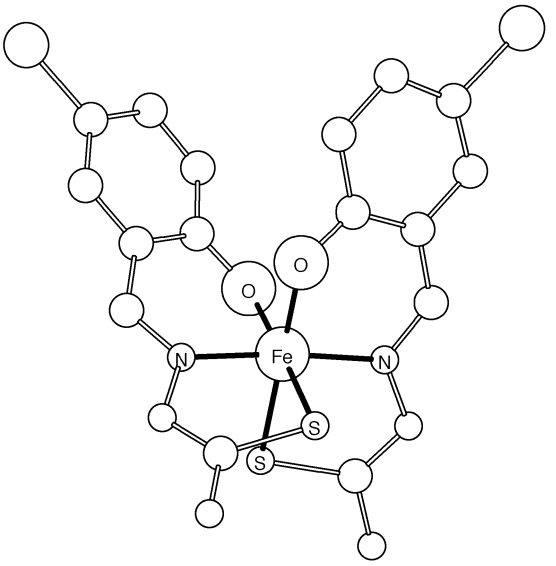

Fig. 2 Structure proposed for the [Fe(5Brthsa)$_2$]$^-$ anion with atom labeling.

that the hydrogen-bond network is very likely to be modified in the course of the spin-crossover process. These data showing the existence of rather strong hydrogen bonds are also in qualitative agreement with the absence of (i) any weight loss due to water removal detected by TGA for temperatures up to 453 K or (ii) any sample alteration during the thermal cycles (including high temperatures) carried out for the vibrational or magnetic measurements. We note that a network of hydrogen bonds interconnecting the ferric complexes is a characteristic common to the hydrated and anhydrous related complexes for which the X-ray crystal structures were solved.[11,19]

Magnetic measurements

The temperature dependence of the $\chi_M T$ product (χ_M being the molar magnetic susceptibility) for the ^{57}Fe-enriched sample **2** is given in Fig. 3 over the 100–380 K temperature range. The plot reveals an $S = 1/2 \leftrightarrow S = 5/2$ spin-crossover of the ferric ion in a pseudo-octahedral symmetry. The transition presents for increasing temperatures a discontinuous character and a broad asymmetric hysteresis centred at $T_c\uparrow \approx 333$ K and $T_c\downarrow \approx 294$ K;

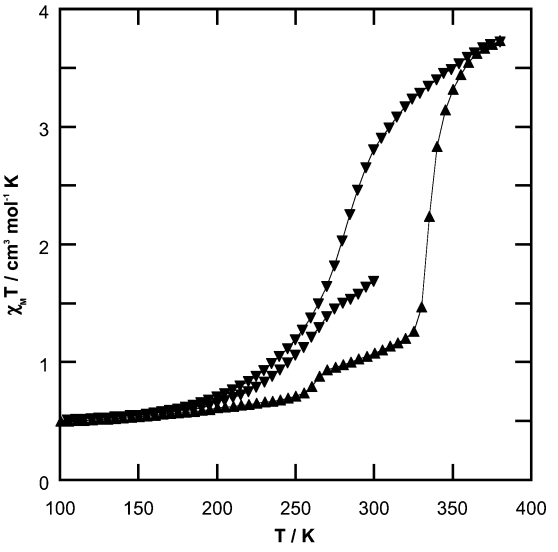

Fig. 3 Temperature dependence of $\chi_M T$ for ^{57}Fe-enriched compound of Li[Fe(5Brthsa)$_2$]·H$_2$O (**2**) (decreasing ▼ and increasing ▲ temperatures).

these values were estimated from the first derivative curves. No complete spin change was attained even at the highest temperature reached (380 K).

During the first thermal cycle (300 to 10 K), the value of $\chi_M T$ decreases from 1.69 cm^3 mol^{-1} K at 300 K to 0.46 cm^3 mol^{-1} K at 10 K, this latter value being indicative of a complete spin conversion at low temperature. On increasing the temperature from 10 to 380 K, the $\chi_M T$ value slightly varies near 260 K, then abruptly increases up to 3.74 cm^3 mol^{-1} K at 380 K. If the solid is cooled again, $\chi_M T$ smoothly decreases down to 0.46 cm^3 mol^{-1} K at 10 K, conferring to this hysteresis loop an asymmetrical shape. It should be noted that the inner branch of the hysteresis loop only occurs on the first cooling step from 300 to 50 K, subsequent cycling of the sample giving rise to the ascending and falling branches previously described.

Effect of crystallinity. The general characteristics of the spin-crossover process were also observed for the more crystalline sample **1**. From the first scanning of the hysteresis loop, the salient features are: (i) a narrower hysteresis loop for **1** ($T_c\uparrow \approx 329$ K, $T_c\downarrow \approx 292$ K) than for **2** ($T_c\uparrow \approx 333$ K, $T_c\downarrow \approx 294$ K) and (ii) a much more discontinuous branch both in the heating and the cooling mode for the more crystalline compound. The intensity of the peak at $T_c\uparrow \approx 260$ K, which corresponds to the small step observed for both compounds in the ascending branch, is reduced in the most crystalline sample. Consequently, such a step is likely to result from another solid phase present as an impurity.

Effect of cycling the sample. Cycling the more crystalline sample **1** three times between 100 and 380 K enables us to ascertain that the sample undergoes no major modification. The hysteresis loop is retained after each complete cycle. The general features due to the development of defect and/or some cracking of the crystallites on passing the crystallographic transition[21] (*vide infra*) have been observed (*i.e.*, a slight broadening of the hysteresis loop, a small lowering and raising of $\chi_M T$ at high and low temperatures, respectively).

An unusual observation in the experimental $\chi_M T(T)$ data is the inner branch recorded upon the first cooling of the sample from room temperature. This curve, localised within the hysteresis loop, is likely to result from a particular mixture of phases that comes from the conditions used for the synthesis. It is to be noted that the crystallisation of the sample takes place over a temperature range located within the hysteresis loop. The X-ray diffraction pattern recorded at room temperature before cooling down the solid shows the coexistence of patterns identified as those of the prevailing low temperature phase and also the high temperature phase.

The hysteresis loop presents an asymmetric shape mostly due to the smoother variation of the falling branch, which deviates from the almost rectangular loop sometimes reported.[11] This feature, described for several compounds,[22–25] may arise from the well-documented effect of the defect structure on the magnetic properties of spin-transition complexes.[9] This should be favoured for solvates, which may provide additional defects from orientational or position disorder or the loss of a small amount of solvent molecules.[23] Another possible origin could be an out-of-equilibrium state of the system. This explanation has been ruled out by some Mössbauer experiments carried out as a function of time (*vide infra*).

Finally, this magnetic behaviour can be compared to the one of the unsolvated salt Li[Fe(5Brthsa)$_2$]. A gradual spin-crossover process without any hysteresis[14] has been reported for this compound, which depends to a large extent on the thermal treatment and also on the air exposure of the sample. This set of observations, only characterised for Li[Fe(5Brthsa)$_2$], confirms that the samples originate from different polycrystalline species. In addition, the strong cooperative interactions responsible for the abrupt transformation and the hysteresis effect of Li[Fe(5Brthsa)$_2$]·H$_2$O are ascribed to the particular structural properties described later (a crystallographic phase transition, the number of structural defects) and to the presence of hydrogen-bonding interactions involving the solvate. It has been noted that in this series of compounds the water of crystallisation leads to additional stabilisation of the LS ferric ion.[15]

Mössbauer measurements

Mössbauer spectra for the ^{57}Fe-enriched sample of Li[Fe(5-Brthsa)$_2$]·H$_2$O (**2**) were recorded in the 4–360 K temperature range. Fig. 4 shows four selected spectra recorded in the heating and cooling modes between 77 and 360 K. The doublet in

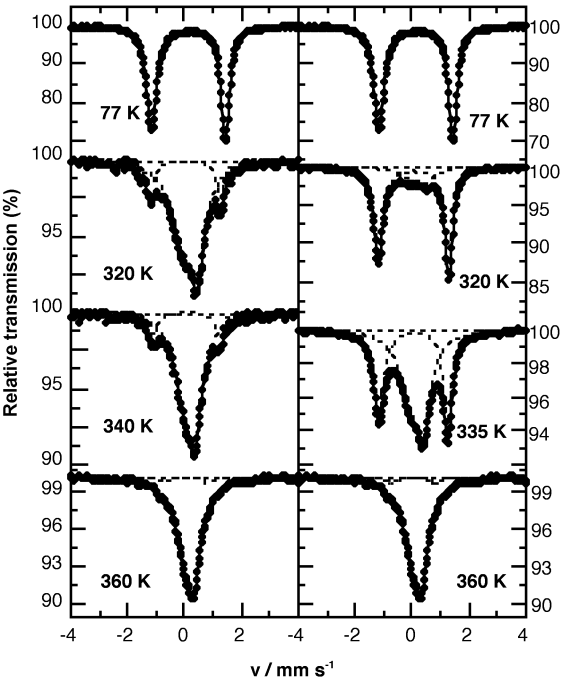

Fig. 4 ^{57}Fe Mössbauer spectra of sample **2** at 77, 320, 335 (340) and 360 K. Measurements were performed in the heating (right) and cooling (left) modes. The transition is centred at *ca.* 313 K.

Table 1 Iron-57 Mössbauer fitting parameters for Li[Fe(5Brthsa)$_2$]·H$_2$O (**2**)

T/K	$\delta^{IS}(^2T_2)$/ mm s^{-1} [a] [b]	$\Delta E_Q(^2T_2)$/ mm s^{-1}	$\Gamma(^2T_2)$/mm s^{-1} [b]		$\delta^{IS}(^6A_1)$/ mm s^{-1} [a] [b]	$\Delta E_Q(^6A_1)$/ mm s^{-1} [b]	$A(^6A_1)$/ A_{tot}	Ln(A_{tot})	γ_{HS}
4	0.267(1)	2.591(2)	0.203(2)	0.214(2)	–	–	–	2.50	0
40	0.266(1)	2.586(2)	0.210(2)	0.221(2)	–	–	–	2.49	0
77	0.262(1)	2.584(2)	0.194(2)	0.210(2)	–	–	–	2.40	0
260	0.207(1)	2.536(2)	0.176(2)	0.201(2)	*0.328*	*0.6*	0.08(2)	1.97	0.11(2)
320	0.180(1)	2.466(1)	0.168(1)	0.199(2)	*0.328*	*0.6*	0.18(2)	1.73	0.26(2)
335	0.176(1)	2.401(2)	0.181(2)	0.212(2)	0.292(1)	0.477(3)	0.59(2)	1.57	0.69(2)
360	*0.176*	1.56(4)	*0.202*	*0.244*	0.294(2)	0.338(6)	0.95(2)	1.29	0.97(2)
320	0.17(1)	2.43(1)	0.18(1)	0.24(2)	0.290(4)	0.575(7)	0.84(2)	1.55	0.89(2)
280	0.205(2)	2.458(3)	0.190(4)	0.235(5)	0.31(1)	0.65(3)	0.58(2)	1.64	0.68(2)
260	0.208(1)	2.523(2)	0.177(2)	0.205(2)	*0.328*	*0.6*	0.19(2)	1.78	0.27(2)
160	0.245(1)	2.559(1)	0.181(1)	0.201(2)	*0.328*	*0.6*	0.02(2)	1.84	0.03(2)

[a] Isomer shifts are relative to Fe metal. [b] Italicised values were fixed in fitting.

the spectrum at 77 K, characterised by a quadrupole splitting $\Delta E_Q = 2.584 \pm 0.002$ mm s^{-1} and an isomer shift $\delta^{IS} = +0.262 \pm 0.001$ mm s^{-1}, is ascribed to the LS $^2T_2$ ground state of iron(III). The broad asymmetric spectrum observed at 360 K was least-squares fitted to two Lorentzian lines constrained to have equal areas. An asymmetric broadening with Lorentzian lineshape is usually attributed to the effect of the magnetic hyperfine interaction, with the spin-flip frequency in small excess to the hyperfine frequency ($\approx 10^8$ Hz). The corresponding parameter values $\Delta E_Q = 0.338 \pm 0.006$ mm s^{-1} and $\delta^{IS} = +0.294 \pm 0.002$ mm s^{-1} are consistent with a HS state of iron(III). The values for the parameters for both the LS and HS states are slightly lower than the corresponding values observed for complexes with [Fe^{III}N$_2$O$_2$S$_2$] coordination cores in the LS state ($\Delta E_Q = 2.7$–3.1 mm s^{-1}; $\delta^{IS} = 0.14$–0.34 mm s^{-1}) or in the HS state ($\Delta E_Q = 0.4$–0.8 mm s^{-1}; $\delta^{IS} = 0.34$–0.54 mm s^{-1}).[10,26] A small fraction of LS state ($\gamma_{LS} \approx 0.03$) was identified at 360 K. Weaker asymmetries in the low-spin spectra are due to the dynamic effect of the magnetic hyperfine interaction involving a smaller spin value.[27]

In the temperature range of 160–360 K the superposition of two distinct quadrupole doublets is observed. These doublets are typical of the HS and LS contributions previously analysed, with marked asymmetrical shapes. This indicates, in a first approach, that the interconversion between the LS and HS states is slow relative to the hyperfine frequencies ($\approx 10^8$ Hz) associated with the nuclear energy schemes. The quadrupole doublets show both marked intensity and linewidth asymmetries in the temperature range for which they coexist in sizeable amounts. For instance, the spectrum at 335 K contains almost equal areas of both states with a high-spin fractional area a_{HS} estimated as 0.59, a value slightly different from the atomic fraction γ_{HS} as discussed further on. The fitted Mössbauer parameters are listed in Table 1 for both increasing and decreasing temperatures.

The thermal behaviour of the HS fraction can be readily deduced from the variation of the area ratio $a_{HS} = A_{HS}/A_{tot}$ (A being the baseline corrected area of the components). Evidence for a difference between the Lamb-Mössbauer factors f (*i.e.*, recoil-free fractions) associated with the two spin states is provided by the variation of Ln(A_{tot}) *vs.* T plotted in Fig. 5. The straight lines stand for the "high temperature approximation" in the Debye model[28,29] [$\mathrm{Ln}(f) = -6E_0^2T / (2k_BMc^2\theta_D^2)$ with $A_{tot} = \mathrm{Cst} \times f$, $E_0 = 14.4$ KeV, M mass of the ^{57}Fe nucleus, θ_D Debye temperature], best fitted to the data, for the pure LS state (full line) and the pure HS state (dotted line). Note that these lines are constrained to intersect at $T = 0$ K ($f = 1$ at $T = 0$ K irrespective of the Debye temperature for this approximation). The ratio of the f_{LS} and f_{HS} values is readily derived at each temperature. A mean value of f_{LS}/f_{HS} of ≈ 1.55 is estimated from these data in the temperature range of 280–350 K and is used for the accurate determination of the HS fraction γ_{HS} from the fractional area, according to: $\gamma_{HS} = [a_{HS}(f_{LS}/f_{HS})]/[(1 - a_{HS}) + a_{HS}(f_{LS}/f_{HS})]$. Fig. 6 shows the temperature dependence of the so-determined HS fraction. The transition is found to take place with an hysteresis loop characterised by $T_c\uparrow = 332$ K (Mössbauer), $T_c\downarrow = 274$ K (Mössbauer) and $\Delta T_c = T_c\uparrow - T_c\downarrow = 58$ K (Mössbauer) after corrections due to the small amount of another phase ($\approx 12.0\%$) giving a step at 260 K (see Fig. 3).

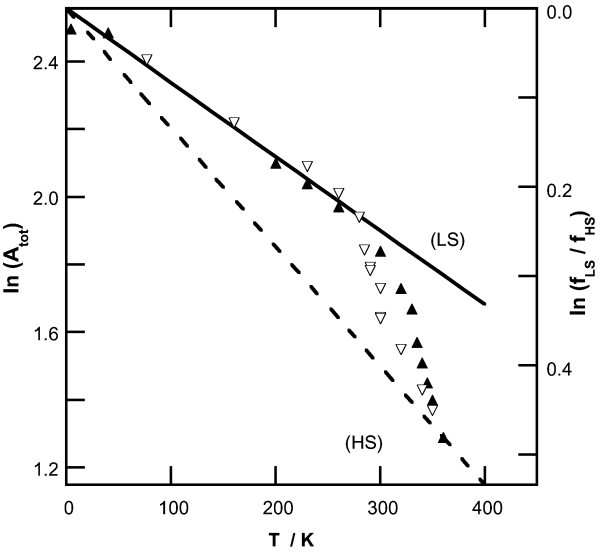

Fig. 5 Temperature dependence of Ln(A_{tot}). Measurements are for both increasing (▲) and decreasing (▽) temperatures.

The comparison of the data obtained by Mössbauer and magnetic susceptibility measurements has been achieved by estimating γ_{HS} from $\gamma_{HS} = (\chi_M T - \chi_M T_{LS})/(\chi_M T_{HS} - \chi_M T_{LS})$ with $\chi_M T_{HS} = 4.377$ (5.92 μ_B) and $\chi_M T_{LS} = 0.5$ cm^3 mol^{-1} K (2.0 μ_B) for the pure HS and LS states, respectively (Fig. 6).[2] In the low temperature region, the variations of γ_{HS} *vs.* T can be superimposed but at high temperature, some deviations are observed, especially in the falling branch of the hysteresis loop. Actually, the $\chi_M T$ value at 380 K ($\chi_M T = 3.74$ cm^3 mol^{-1} K, $\gamma_{HS} \approx 0.84$) suggests that the spin transition of the metal ion is not fully completed, whereas γ_{HS} values close to unity are evaluated by Mössbauer spectrometry in this range of temperature (340 → 360 → 310 K).

Some discrepancies can be ascribed to different reasons: (i) the unusual broadening of the Mössbauer lines (as discussed later) in the temperature range of the transition, (ii) the release of water molecules that may be favoured in the Mössbauer experimental conditions (dynamic secondary vacuum

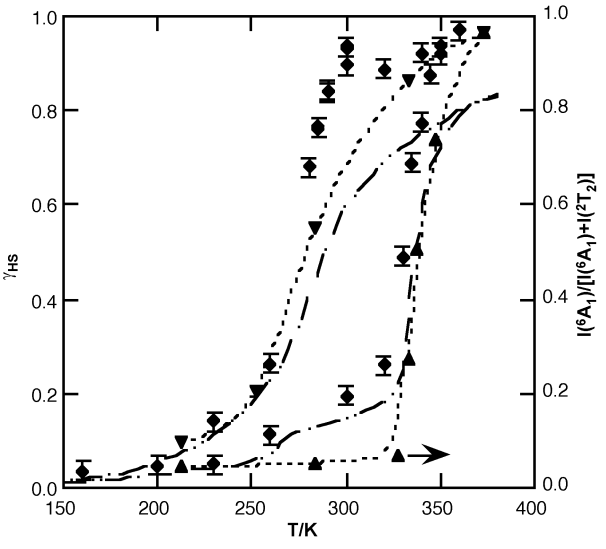

Fig. 6 Temperature dependence of the HS fraction γ_{HS} (◆) for compound **2** deduced from the fractional area a_{HS} of the Mössbauer components (see text). Temperature dependence of the area fraction (▲, ▼), $\sigma = I(^6A_1)/[I(^6A_1) + I(^2T_2)]$, from the peak profiles of the Bragg reflections at 13.20° ($^2T_2$) and 14.00° ($^6A_1$). The values of γ_{HS} calculated from $\chi_M T(T)$ are reported for **2** (–·–).

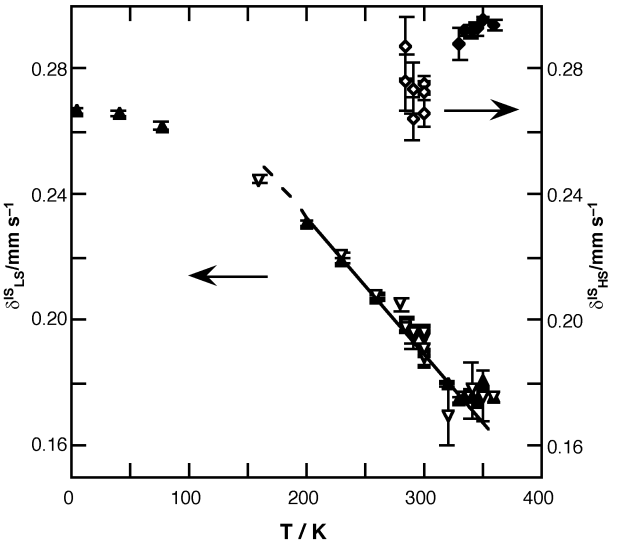

Fig. 7 Temperature dependence of the isomer shift $\delta^{IS}(T)$ for the HS ($^6A_1$) and the LS ($^2T_2$) states at increasing (◆,▲) and decreasing (◇,▽) temperatures. The error bars are marked only when larger than the size of the symbol. The straight line has been fitted to the LS data to determine the effective mass involved in the second-order Doppler shift.

$\sim 10^{-6}$ torr, very slow scan rates). This second hypothesis cannot be fully discarded although a $\chi_M T$ *vs.* T measurement performed on a thermally treated sample of Li[Fe(5Brthsa)$_2$]·H_2O did not allow us to detect any major modification of the hysteresis loop.[30]

As previously mentioned, the asymmetrical shape of the hysteresis loop might also originate from an out-of-equilibrium state of the system giving rise to a kinetic process and a marked time dependence of the physical measurements at fixed values of the temperature.[12a,b,23] Accordingly, the time dependence of the Mössbauer spectra has been recorded at fixed temperatures over several days for different states belonging to the descending branch of the hysteresis loop (in the temperature range 300–280 K). However, the absence of any detectable time dependence of the areas of the Mössbauer components has ruled out such an explanation.

The temperature dependence of the isomer shifts $\delta^{IS}(T)$ is displayed in Fig. 7. The analysis of the isomeric shift through the Debye model of the lattice dynamics[12,28] leads to an effective mass value $M_{eff} = 97$ g mol^{-1} [$d(\delta^{IS})/dT = -4.270 \times 10^{-4}$ mm s^{-1} K^{-1}] associated with the vibrational modes of the LS iron atom. Due to the strength of the Fe–N bonds, this mass is significantly larger than that of the single iron atom (57 g mol^{-1}). By taking advantage of the so-determined M_{eff} value, the experimental value of the slope in the LS state [dLn$(A_{tot})/dT = -2.19 \times 10^{-3}$ K^{-1}] leads to a rather high value of $\theta(LS) \approx 191$ K, which reveals a relatively high degree of rigidity of the lattice. The occurrence of the LS-to-HS transition results in a decrease of the Lamb–Mössbauer factor, assigned to (as a major factor) the decrease in the effective mass due to the weakening of the chemical bond around the iron atom.[24] Following this viewpoint, a value of $M_{eff} \sim 60$ g mol^{-1} is derived for the HS state.

The rather slow spin-state interconversion rates (relative to the Mössbauer time scale) observed for this ferric thiosemicarbazone complex may account for the significant changes of the coordination polyhedron accompanying the spin-crossover process, in agreement with the variation of the effective masses.[8] It should be noted, however, the sizeable broadening of the Mössbauer lines, mainly of the HS lines, when both components coexist in large amounts. This suggest some dynamical mixing of the lines,[31] which obviously adds to the magnetic relaxation effect already responsible for the asymmetric broadening of the HS doublet.

The complete investigation of the quadrupole splitting and isomer shift values has revealed features that are not all consistent with the expected trends. These features are: (i) the HS isomer shift values are not a decreasing function of temperature, (ii) the HS quadrupole splitting values are not temperature-independent and (iii) the LS quadrupole splitting values change very rapidly in the transition temperature range. These discrepancies could be explained by the presence of an additional HS phase, which becomes the dominent HS contribution below ~300 K, and is probably responsible for the "minor" transition displayed at ~260 K by the magnetic data in Fig. 1. Due to the presence of this additional phase, any further analysis of the Mössbauer data would be far too speculative.

Calorimetric measurements

The DSC curves obtained for the more crystalline sample **1** at a scan rate of 10 K min^{-1} are shown in Fig. 8. For samples **1** and **2**, the observed areas under the peaks corresponding to the heating and cooling cycles were found to be equal within experimental error (±5%) for samples **1** and **2**. In the heating mode, the transformation $^2T_2 \rightarrow {}^6A_1$ is characterised by a rather sharp endothermic peak ($T_{onset} = 323 \pm 0.5$ K, $T_{max} = 330.4 \pm 0.5$ K). In the cooling mode, the broader exothermic peak corresponding to the transformation $^6A_1 \rightarrow {}^2T_2$ is centred around 291 K ($T_{onset} \approx 304$ K). The observations of a well-defined endothermic peak and a rather broad exothermic peak are consistent with the thermal hysteresis characterised by the magnetic measurements. The average value of the enthalpy variations obtained for a number of measurements carried out at increasing temperatures is found to be $\Delta H = 5.7 \pm 0.5$ kJ mol^{-1} after correction for the presence of a small amount of another phase corresponding to the step at 260 K. The derived value of the entropy variation calculated with the average of the two T_{onset} temperatures at 313 K is $\Delta S = 18 \pm 2$ J mol^{-1} K^{-1}. The changes of enthalpy ΔH and entropy ΔS associated with the spin transition of Schiff-base ferric complexes have only rarely been determined from calorimetric measurements.[32,33] They have been found to vary

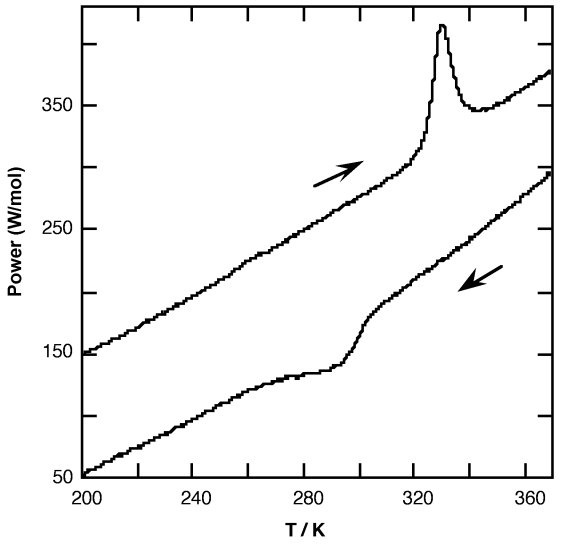

Fig. 8 DSC curves obtained for **1** at a scan rate of 10 K min^{-1}.

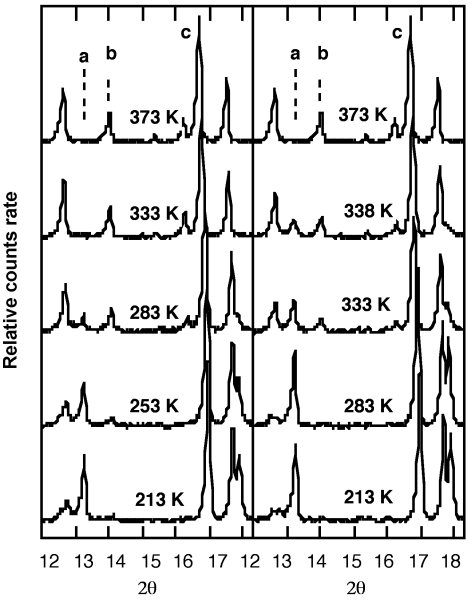

Fig. 9 X-Ray diffraction peak profiles of sample **1** within the range $12° < 2\theta < 18.3°$ as a function of temperature. The temperatures correspond to the ascending (right) and descending (left) branches of the hysteresis loop.

within the range of 5–8 kJ mol^{-1} and 34–41 J mol^{-1} K^{-1}, respectively. In this study, the value of ΔS (18 J mol^{-1} K^{-1}) is considerably smaller than the previous ones but compares with the results published by Shipilov *et al.* for ferric thiosemicarbazone complexes (16–18 J mol^{-1} K^{-1}).[34] As expected, this entropy variation is larger than the electronic contribution $R\mathrm{Ln}(6/2) = 9.13$ J mol^{-1} K^{-1} resulting from the difference in the spin degeneracies of the HS ($S = 5/2$) and LS ($S = 1/2$) states. The excess of entropy [*i.e.*, $\Delta S - R\mathrm{Ln}(3)$] is provided by the vibrational entropy term related to both intramolecular vibrations (main contribution) and lattice vibrations. The small value deduced from these data might be indicative of (i) minor changes in the [$FeN_2O_2S_2$] coordination polyhedron associated to the LS $\leftrightarrow$ HS transition or (ii) an additional positive or negative contribution to the lattice entropy due to the change of hydrogen-bonding interactions.[18c] In contrast, an order-disorder transition, which cannot be excluded at this stage of the work, would result in a positive entropy term.

X-Ray powder diffraction

The X-ray diffraction patterns of a crystalline sample of Li[Fe(5Brthsa)$_2$]·H_2O (**1**) have been recorded over the temperature range from 213 to 373 K. Fig. 9 shows selected diffraction patterns limited to the diffraction angles 2θ between 12.00° and 18.30°. A number of lines, for example those centred at $2\theta \approx 13.28°$ (labelled a) and 14.03° (labelled b), are assigned to the low-spin phase (at 213 K) and to the high-spin phase (at 373 K), respectively. These lines co-exist and exhibit opposite intensity variations as the temperature varies. The most intense line of the pattern (labelled c, at 213 K) located at ≈16.99° appears to be simply shifted towards lower angle values by increasing the temperature. A more detailed analysis clearly shows several ranges of variation depending on the temperature. From 213 to 283 K, a linear variation of d_{hkl} is assigned to the LS phase of the crystal lattice (thermal expansion). Between 333 and 343 K, the slight broadening of the c line unambiguously demonstrates the occurrence of structural reorganisation. At higher temperatures, a different monotonous variation characterises the HS phase. In the cooling mode, the observation of broadened lines at 283 and 263 K is attributed to the superposition of the close individual lines due to the LS and HS phases. These results clearly establish that this process can be classified as a crystallographic first-order phase transition.

The relative area of an HS line $I(^6A_1)/[I(^6A_1) + I(^2T_2)]$ *vs.* temperature is displayed in Fig. 6. This parameter is evaluated from the areas of the diffraction lines at 13.28° [line a, $I(^2T_2)$] and 14.03° [line b, $I(^6A_1)$], which are slightly dependent on the background and unsplit. Fig. 6 does not show the step displayed by the magnetic measurements at 260 K. This is due to the particular choice of pure diffraction lines, which do not contain any contribution of the other solid phase already suspected. In agreement with the DSC, magnetic and Mössbauer effect studies, the crystallographic phase transition is found to present a hysteresis effect ($T_c\uparrow = 338$ K and $T_c\downarrow = 279$ K). It can be inferred that the spin-state interconversion of the ferric ion is concurrent and hence coupled to the phase transition of the lattice.

Summary

We have characterised a discontinuous spin transition of a ferric complex with a rather large hysteresis centred near room temperature. The cooperative character of this transformation is ascribed to a crystallographic first-order phase transition. The modification of a hydrogen-bond network between the water of crystallisation and ferric complexes might account for this phase transition.

It is well-established that the observation of cooperative intermolecular interactions and hysteresis effect are of interest for potential applications based either on thermal bistability or optical switching processes. Evidence of an LIESST effect have been very recently provided for a ferric compound.[12c] Interest in such molecules would be heightened by the additional observation of the so-called LD-LISC effect. Thus, the properties of a ferric complex analogous to the one presently investigated but containing photoisomerisable groups are also currently under investigation.

Experimental

Syntheses

Thiosemicarbazide and 5-bromosalicylaldehyde were purchased from ACROS. LiOH·H_2O was purchased from Janssen Chimica and $Fe(NO_3)_3$·$9H_2O$ from Fluka. Synthesis of 5-bromosalicylaldehyde thiosemicarbazone, hereafter designed by

H_2-5Brthsa, was according to the method previously described.[20] Yield 75%. 1H NMR (250 MHz, [D6]-DMSO, 20 °C, TMS): $\delta = 11.41$ (s, 1H), 10.25 (br s, 1H), 8.26 (s, 1H), 8.2–8.1 (m, 2H), 7.23 (dd, 1H), 6.80 (d, 1H). Anal. calcd (%) for $C_8H_8N_3OSBr$ (274,13 g mol^{-1}): C 35.17, H 2.95, N 15.39, S 11.71, O 5.86; found C 35.09, H 2.95, N 15.71, S 11.69, O 5.86. IR (KBr): 3455 (ν_{OH}), 3250–2997 (ν^{as} and ν^{s}_{NH2}), 3161 (ν_{NH}), 1653 (δ_{NH2}), 1610, 1601 ($\nu_{C=N}^{azomethyne}$ and $\nu_{C=C}$), 1545 ($\nu_{amide\ II}$), 1294 ($\nu_{amide\ III}$), 1264 (ν_{CO}), 1064 ($\nu_{C=S}$), 777 (ν^{s}_{CS}) cm^{-1}.

Li[Fe(5Brthsa)$_2$]·H$_2$O (1). The Schiff-base ligand H_2-5Brthsa (700 mg, 2.55 mmol) and LiOH·H_2O (214 mg, 5.10 mmol) were first reacted in 40 mL of water at 100 °C. An aqueous solution (20 mL) of $Fe(NO_3)_3$·$9H_2O$ (515 mg, 1.27 mmol) was added very slowly to this refluxed mixture. After 30 min of stirring, the hot solution was allowed to cool to room temperature overnight. The black crystalline compound was filtrered off, washed with water and dried in vacuum, first at room temperature, then at 50 °C overnight. Yield 100%. Anal. calcd (%) for $C_{16}H_{14}N_6O_3S_2Br_2FeLi$ (622.8 g mol^{-1}): C 30.83, H 2.27, N 13.49, S 10.27, Fe 8.93; found C 30.76, H 2.25, N 13.52, S 10.08, Fe 8.32. ES-MS (MeOH): $m/z = 599.9$ ($[Fe(C_8H_6N_3OSBr)_2]^-$). IR (KBr, 150 K): 3504, 3485, 3446, 3430 (ν^{as} and ν^{s}_{OH}), 3314–2996 (ν^{as} and ν^{s}_{NH2}), 1665, 1627, 1624, 1618 (δ_{NH2} and δ_{HOH}), 1610 ($\nu_{C=C}$ and $\nu_{C=N}$), 1588 ($\nu_{C=N}^{azomethyne}$), 1512 ($\nu_{amide\ II}$), 1271 (ν_{CO}), 758 (ν^{s}_{CS}), 574 ($\nu_{metallacycle}$ containing Fe–S) cm^{-1}. IR (380 K): 3489, 3451 (ν^{as} and ν^{s}_{OH}), 3292, 3151 (ν^{as} and ν^{s}_{NH2}), ~1643 (δ_{NH2} or δ_{HOH}), 1607, 1587 ($\nu_{C=C}$ and $\nu_{C=N}^{azomethyne}$), 1538 ($\nu_{amide\ II}$), 1283 (ν_{CO}), 535 ($\nu_{metallacycle}$ containing Fe–S) cm^{-1}.

Synthesis of the ^{57}Fe-enriched sample (2). A sample of Li[Fe(5Brthsa)$_2$]·H_2O enriched to 26% in ^{57}Fe was prepared by dissolving 4.1 mg of 90% enriched ^{57}Fe (0.072 mmol) and 10.9 mg of Fe powder (0.194 mmol) in 3 mL of concentrated HNO_3 at 60–70 °C for 2 h. The excess of nitric acid was removed under reduced pressure by several washing with water to give a solid orange residue. The solid was dissolved in water (5 mL) and slowly added to a mixture of H_2-5Brthsa (147.2 mg, 0.537 mmol) and LiOH·H_2O (45 mg, 1.07 mmol) in water (9 mL) at 90 °C. After additional stirring for 30 min at 90 °C, the solution was allowed to cool to room temperature. The microcrystalline solid was filtered off, washed with water and dried in vacuum. Anal. found (%): C 30.68, H 2.14, N 13.64, S 10.46, Fe 8.63.

Physical measurements and instrumentation

^{1}H NMR spectra were recorded on a Bruker AM 250 (250 MHz) spectrometer. The ES-MS spectrum was recorded from a 2×10^{-4} M methanol solution of the complex on a Finnigan-Mat SSQ 700 spectrometer. FTIR spectra were obtained on a Perkin–Elmer spectrum 1000 spectrometer equipped with the Eurolabo variable temperature cell (21 525) and Specac temperature controller (20 120) for temperature variable measurements. The thermal analysis was carried out in the 293–383 K temperature range under ambient atmosphere. A sample of Li[Fe(5Brthsa)$_2$]·H_2O (58 mg) was characterised.

Magnetic susceptibility measurements. The temperature dependence of the magnetic susceptibility was characterised with a Quantum Design SQUID Magnetometer (MPMS5S Model) calibrated against a standard palladium sample. The independence of the susceptibility value with regard to the applied magnetic field was checked at room temperature.

^{57}Fe Mössbauer measurements. The Mössbauer spectra were recorded on a constant-acceleration spectrometer, with a 25 mCi source of ^{57}Co in rhodium matrix. The polycrystalline absorber contained 35 mg of material per cm^2 (*i.e*, ≈0.83 mg cm^{-2} of ^{57}Fe). Variable-temperature spectra, in the 360–160 K range, were obtained by using a standard bath cryostat; the temperature was controlled by a linear sensor calibrated at 4.2 and 273 K. After folding of the spectra, the typical experimental linewidth, in the considered velocity range, is $\Gamma_{exp} = 0.215$ mm s^{-1}. The spectra were fitted without correction for the thickness effect. Least-squares-fitted parameters are given with their standard deviation of statistical origin (in parentheses) and isomer shift values refer to metallic iron at room temperature. Accordingly, the isomer shift data previously published[10,26] for similar ferric complexes have been rescaled to metallic iron reference by the negative correction (*i.e.*, δ_{lit} −0.258 mm s^{-1}).

Differential scanning calorimetry measurements. Calorimetric experiments were performed on a Perkin–Elmer DSC 2 adapted to low temperatures. A laboratory-made cooling device permitted a lowest starting temperature of 80 K. Calibration was performed with standard organic liquids. The solid–solid and normal melting transitions of cyclohexane were reproduced with an accuracy of 0.5 K and 10% of the enthalpies, which are typical values for such experiments. Calorimetric data were recorded on heating or cooling at a rate of 10 K min^{-1} between 150 and 380 K. Aluminium sample holders were loaded with ≈10 mg of compound and sealed under ambient atmosphere.

Powder X-ray diffraction patterns. These were recorded on a Siemens D500 vertical scan diffractometer equipped with a scintillation detector and a rear monochromator ($CuK\alpha_1$, $\lambda = 1.5405$ Å). All diffraction lines (reflection mode) were recorded with an accuracy of 0.02°. Solid samples were placed in a copper–tin alloy sample holder. The apparatus was calibrated at room temperature with respect to quartz previously annealed at 1173 K. The temperature controlled by a liquid nitrogen cooling system (Anton Paar KG) was measured by means of a Pt100 platinum probe.

Acknowledgements

We thank Jean-Paul Audière for TGA measurements, Ary Dworkin, Hassan Allouchi and Michel Gasgnier for preliminary DSC and powder XRD measurements, and Jacqueline Zarembowitch and René Clément for very fruitful discussions. Financial support from the research fund TMR of the European Community (Contract No. ERB-FMRX-CT98-0199) is gratefully acknowledged.

References

1 L. Cambi and A. Cagnasso, *Atti. Accad. Naz. Lincei, Cl. Sci. Fis., Mat. Natur. Rend.*, 1931, **13**, 809.
2 O. Kahn, *Molecular Magnetism*, VCH, New York, 1993.
3 P. Gütlich, A. Hauser and H. Spiering, *Angew. Chem., Int. Ed. Engl.*, 1994, **33**, 2024.
4 M. Sorai, J. Ensling, K. M. Hasselbach and P. Gütlich, *Chem. Phys.*, 1977, **20**, 197.
5 (*a*) E. König and G. Ritter, *Solid State Commun.*, 1976, **18**, 279; (*b*) E. König, G. Ritter, W. Irler and H. A. Goodwin, *J. Am. Chem. Soc.*, 1980, **102**, 4681.
6 W. Vreugdenhil, J. H. van Diemen, R. A. G. de Graaff, J. G. Haasnoot, A. M. van der Kraan, O. Kahn and J. Zarembowitch, *Polyhedron*, 1990, **9**, 2971.
7 (*a*) J. Zarembowitch and O. Kahn, *New J. Chem.*, 1991, **15**, 181; (*b*) J. Kröber, E. Codjovi, O. Kahn, F. Grolière and C. Jay, *J. Am Chem. Soc.*, 1993, **115**, 9810; (*c*) O. Kahn and C. Jay Martinez, *Science*, 1998, **279**, 44.
8 (*a*) H. Oshio, K. Toriumi, Y. Maeda and Y. Takashima, *Inorg. Chem.*, 1991, **30**, 4252; (*b*) M. F. Tweedle and L. J. Wilson, *J. Am. Chem. Soc.*, 1976, **98**, 4824.

9 (*a*) M. S. Haddad, M. W. Lynch, W. D. Federer and D. N. Hendrickson, *Inorg. Chem.*, 1981, **20**, 123; (*b*) M. S. Haddad, W. D. Federer, M. W. Lynch and D. N. Hendrickson, *Inorg. Chem.*, 1981, **20**, 131.

10 (*a*) V. V. Zelentsov, *Sov. Sci. Rev. B, Chem.*, 1987, **10**, 485; (*b*) V. V. Zelentsov, *Koord. Khim.*, 1992, **18**, 787.

11 (*a*) M. D. Timken, S. R. Wilson and D. N. Hendrickson, *Inorg Chem.*, 1985, **24**, 3450; (*b*) M. Mohan, P. H. Madhuranath, A. Kumar and N. K. Jha, *Inorg. Chem.*, 1989, **28**, 96; (*c*) N. S. Gupta, M. Mohan, N. K. Jha and W. E. Antholine, *Inorg. Chim. Acta*, 1991, **184**, 13.

12 (*a*) H. Oshio, K. Kitazaki, J. Mishiro, N. Kato, Y. Maeda and Y. Takashima, *J. Chem. Soc., Dalton Trans.*, 1987, 1341; (*b*) S. Hayami and Y. Maeda, *Inorg. Chim. Acta*, 1997, **255**, 181; (*c*) S. Hayami, Z. Z. Gu, M. Shiro, Y. Einaga, A. Fujishima and O. Sato, *J. Am. Chem. Soc.*, 2000, **122**, 7126; (*d*) S. Hayami, Z. Z. Gu, H. Yoshiki, A. Fujishima and O. Sato, *J. Am. Chem. Soc.*, 2001, **123**, 11 644.

13 (*a*) M.-L. Boillot, C. Roux, J.-P. Audière, A. Dausse and J. Zarembowitch, *Inorg. Chem.*, 1996, **35**, 3975; (*b*) M.-L. Boillot, S. Chantraine, J. Zarembowitch, J.-Y. Lallemand and J. Prunet, *New J. Chem.*, 1999, **23**, 179; (*c*) A. Sour, M.-L. Boillot, E. Rivière and P. Lesot, *Eur. J. Inorg. Chem.*, 1999, 2117.

14 V. V. Zelentsov, L. G. Bogdanova, A. V. Ablov, N. V. Gerbeleu and C. V. Dyatlova, *Russ. J. Inorg. Chem. (Transl. of Zh. Neog. Khim.)*, 1973, **18**, 1410.

15 V. V. Zelentsov, V. M. Mokshin, S. S. Sobolev and V. I. Shipilov, *Dokl. Akad. Nauk. SSSR*, 1984, **277**, 900.

16 V. V. Zelentsov, A. V. Ablov, K. I. Turta, R. A. Stukan, N. V. Gerbeleu, E. V. Ivanov, A. P. Bogdanov, N. A. Barba and V. G. Bodyu, *Russ. J. Inorg. Chem. (Transl. of Zh. Neog. Khim.)*, 1972, **17**, 1000.

17 A. V. Ablov and N. V. Gerbeleu, *Russ. J. Inorg. Chem. (Transl. of Zh. Neog. Khim.)*, 1965, **10**, 33.

18 (*a*) *Infrared and Raman Spectra of Inorganic and Coordination Compounds*, ed. K. Nakamoto, John Wiley & Sons, Inc., New York, 1986; (*b*) *The Infra-red Spectra of Complex Molecules*, ed. L. J. Bellamy, Methuen & Co Ltd., London, 1960; (*c*) *The Hydrogen Bond*, eds. G. C. Pimentel and A. L. McClellan, W. H. Freeman, San Francisco, London, 1960, p. 106; (*d*) C. Collard-Charon and M. Renson, *Bull. Soc. Chim. Belg.*, 1963, **72**, 291; (*e*) M. J. M. Campbell, *Coord. Chem. Rev.*, 1975, **15**, 279; (*f*) A. B. Ilyukhin, V. L. Abramenko and V. S. Sergienko, *Russ. J. Coord. Chem.*, 1994, **20**, 617; (*g*) R. Claude, J. Zarembowitch and M. Philoche-Levisalles, *New J. Chem.*, 1991, **15**, 635.

19 (*a*) N. A. Ryabova, V. I. Ponomarev, V. V. Zelentsov and L. O. Atovmyan, *Sov. Phys. Crystallogr. (Engl. Transl.)*, 1982, **27**, 46; (*b*) N. A. Ryabova, V. I. Ponomarev, V. V. Zelentsov and L. O. Atovmyan, *Sov. Phys. Crystallogr. (Engl. Transl.)*, 1982, **27**, 171; (*c*) N. A. Ryabova, V. I. Ponomarev, V. V. Zelentsov and L. O. Atovmyan, *Sov. Phys. Crystallogr. (Engl. Transl.)*, 1981, **26**, 53; (*d*) N. A. Ryabova, V. I. Ponomarev, V. V. Zelentsov, V. I. Shipilov and L. O. Atovmyan, *J. Struct. Chem.*, 1981, **22**, 234; (*e*) N. A. Ryabova, V. I. Ponomarev, L. O. Atovmyan, V. V. Zelentsov and V. I. Shipilov, *Sov. J. Coord. Chem. (Engl. Transl.)*, 1978, **4**, 95.

20 S. Padhyé and G. B. Kauffman, *Coord. Chem. Rev.*, 1985, **63**, 127.

21 (*a*) E. König, G. Ritter and S. K. Kulshresta, *Chem. Rev.*, 1985, **85**, 219; (*b*) E. König, *Prog. Inorg. Chem.*, 1987, **35**, 527.

22 Y. Garcia, P. J. van Koningsbruggen, R. Lapouyade, L. Fournès, L. Rabardel, O. Kahn, V. Ksenofontov, G. Levchenko and P. Gütlich, *Chem. Mater.*, 1998, **10**, 2426.

23 E. König, G. Ritter, S. K. Kulshreshtha and N. Csatary, *Inorg. Chem.*, 1984, **23**, 1903.

24 E. König, G. Ritter, W. Irler and S. M. Nelson, *Inorg. Chim. Acta*, 1979, **37**, 169.

25 J. Zarembowitch and O. Kahn, *Inorg. Chem.*, 1984, **23**, 589.

26 (*a*) K. I. Turta, A. V. Ablov, N. V. Gerbeleu, R. A. Stukan and C. V. Dyatlova, *Russ. J. Inorg. Chem. (Transl. of Zh. Neorg. Khim.)*, 1975, **20**, 82; (*b*) K. I. Turta, A. V. Ablov, N. V. Gerbeleu, C. V. Dyatlova and R. A. Stukan, *Russ. J. Inorg. Chem. (Transl. of Zh. Neorg. Khim.)*, 1976, **21**, 266; (*c*) A. V. Ablov, R. A. Stukan, K. I. Turta, N. V. Gerbeleu, C. V. Dyatlova and N. A. Barba, *Russ. J. Inorg. Chem. (Transl. of Zh. Neorg. Khim.)*, 1974, **19**, 59.

27 M. D. Timken, A. M. Abdel Mawgoud and D. N. Hendrickson, *Inorg. Chem.*, 1986, **25**, 160.

28 (*a*) *Mössbauer Spectroscopy*, eds. N. N. Greenwood and T. C. Gibb, Chapman and Hall Ltd., London, 1971, p.11; (*b*) *Mössbauer Spectroscopy*, eds. N. N. Greenwood and T. C. Gibb, Chapman and Hall Ltd., London, 1971, p.52.

29 K Boukheddaden and F. Varret, *Hyperfine Interact.*, 1992, **72**, 349.

30 The magnetic measurement was performed before and after a thermal treatment of $Li[Fe(5Brthsa)_2]\cdot H_2O$. This consisted in heating the powder in a quartz holder under dynamic vacuum (360 K, vacuum $\sim 10^{-2}$ torr, 48 h), the sample holder being sealed at this stage to prevent any uptake of water. These χ_M *vs.* *T* measurements reveal a small increase of $\chi_M T$ of ~4% at 360 K but no major modification of the hysteresis loop.

31 (*a*) P. Adler, H. Spiering and P. Gütlich, *Inorg. Chem.*, 1987, **26**, 3840; (*b*) P. Adler, P. Poganiuch and H. Spiering, *Hyperfine Interact.*, 1989, **52**, 47; (*c*) P. Adler, H. Spiering and P. Gütlich, *J. Phys. Chem. Solids*, 1989, **50**, 587; (*d*) A. Bousseksou, C. Place, J. Linares and F. Varret, *J. Magn. Magn. Mater.*, 1992, **104–107**, 225.

32 (*a*) A. J. Conti, R. K. Chadha, K. M. Sena, A. L. Rheingold and D. N. Hendrickson, *Inorg. Chem.*, 1993, **32**, 2670; (*b*) A. J. Conti, K. Kaji, Y. Nagano, K. M. Sena, Y. Yumoto, R. K. Chadha, A. L. Rheingold, M. Sorai and D. N. Hendrickson, *Inorg. Chem.*, 1993, **32**, 2681.

33 M. Sorai, Y. Maeda and H. Oshio, *J. Phys. Chem. Solids*, 1990, **51**, 941.

34 V. I. Shipilov, V. V. Zelentsov, V. M. Zhdanov and V. A. Turdakin, *JETP Lett. Engl. Transl.*, 1974, **19**, 294.